

General Algorithms for 3-D Motion of a Non-Planar Body in a Steady-State Force Field

Ronald M. Pratt
Khairil Mazwan Bin Mohamad Zaini

ABSTRACT

Determining trajectories of objects in three-dimensional space is fundamental to many disciplines. Whether the objects be molecules or celestial bodies, the standard Newtonian equations of motion describe this dynamic behavior. Unfortunately, however, the complexity of a real system normally requires that the equations of motion be solved numerically and methods presented in classical mechanics textbooks are of little practical use. In addition, the standard equations of motion involving Euler angles contain singularities and are therefore not suitable for computer solution. This paper discusses implementation of two powerful but little known techniques using quaternions, the Evans and the Rapaport methods. These little known techniques have been developed by and used for molecular modeling, but their application is far reaching, and can be applied to any system where quantum or relativistic effects may be neglected. These methods show excellent conservation of energy over many millions of time steps and are free of singularities. Herein we compare the two methods in terms of efficiency and accuracy. Due to their general nature, the algorithms may be readily coded to meet the needs of many applications.

Key words: Classical Mechanics, Newtonian, Lagrangian, Quaternions, Euler Equations of Motion, Euler Angles, Predictor-Corrector, Gear

INTRODUCTION

Classical motion of rigid bodies is an ancient topic with diverse applications. The traditional methods have been to model rigid body motion either using constrained equations of translational motion (Ryckaert et al. 1976) or unconstrained equations of motion for both translational and rotation (Sonnenschein 1985). The latter method tends to be more general and easily adapted to both microscopic and macroscopic systems, and is also intuitively more straightforward.

Unfortunately the equations normally developed and presented in classical mechanics textbooks are either suitable only for trivial systems amenable to analytic solution, or at best, the equations presented for numerical solution contain singularities (Allen et al. 1987). In this paper we look at two different implementations of a powerful and general method of setting up and numerically solving the translational and rotational equations of motion using quaternions. A simple, yet sufficiently complex system to fully exercise the power of the quaternion method is taken as a case study.

BACKGROUND

The configuration of any rigid body in 3-dimensional dspace may be given by Cartesian coordinates of the center of mass and by three Euler angles. The former designate the location in space of the object's center of mass, the latter specify the object's orientation. The familiar Euler equations of motion, as found in most textbooks (Goldstein 1980) are given:

$$\begin{aligned}\dot{\phi} &= -\omega_x^s \frac{\sin \phi \cos \theta}{\sin \theta} + \omega_y^s \frac{\cos \phi \cos \theta}{\sin \theta} + \omega_z^s \\ \dot{\theta} &= \omega_x^s \cos \phi + \omega_y^s \sin \phi \\ \dot{\psi} &= \omega_x^s \frac{\sin \phi}{\sin \theta} - \omega_y^s \frac{\cos \phi}{\sin \theta}\end{aligned}\quad (\text{Eq. 1})$$

where ϕ , θ , and ψ represent the three Euler angles, ω_x , ω_y and ω_z represent the angular velocity components, and the "s" superscript indicates that the equations are to be integrated in the space fixed (not body fixed) reference frame. Of course, a rigid body may assume any spatial orientation, but we see from (Eq. 1) that problems will arise when $\sin \theta$ approaches zero (Spiegel 1986). This problem has been ingeniously overcome (Evans 1977) by replacing the three Euler angles with four quaternions, and reformulating the equations of motion in terms of these four new quantities. The four quaternions are defined from the Euler angles:

$$\begin{aligned}q_1 &\equiv \sin \frac{\theta}{2} \cos \frac{\phi - \psi}{2} \\ q_2 &\equiv \sin \frac{\theta}{2} \sin \frac{\phi - \psi}{2} \\ q_3 &\equiv \cos \frac{\theta}{2} \sin \frac{\phi + \psi}{2} \\ q_4 &\equiv \cos \frac{\theta}{2} \cos \frac{\phi + \psi}{2}\end{aligned}\quad (\text{Eq. 2})$$

Since we have introduced four new quantities to replace three, the four quantities are not independent. We therefore have the following relationships (Rapaport 1998):

$$q_1^2 + q_2^2 + q_3^2 + q_4^2 = 1 \quad (\text{Eq. 3})$$

$$q_1 \dot{q}_1 + q_2 \dot{q}_2 + q_3 \dot{q}_3 + q_4 \dot{q}_4 = 0 \quad (\text{Eq. 4})$$

In this paper we will consider both a first order (Evans 1977, 1983) and a second order (Rapaport 1985, 1998) method of solving (Eq. 1) in terms of quaternions. Any numerical integration method can be used, however we will only consider the Gear predictor-corrector method (Haile 1992).

In first order formulation, (Eq. 1) is recast in term of quaternions:

$$\begin{pmatrix} \ddot{q}_1 \\ \ddot{q}_2 \\ \ddot{q}_3 \\ \ddot{q}_4 \end{pmatrix} = \frac{1}{2} \begin{pmatrix} q_4 & -q_3 & q_2 & q_1 \\ q_3 & q_4 & -q_1 & q_2 \\ -q_2 & q_1 & q_4 & q_3 \\ -q_1 & q_2 & -q_3 & q_4 \end{pmatrix} \begin{pmatrix} \omega_x^b \\ \omega_y^b \\ \omega_z^b \\ 0 \end{pmatrix} \quad (\text{Eq. 5})$$

In second order formulation, (Eq. 1) is written:

$$\begin{pmatrix} \ddot{q}_1 \\ \ddot{q}_2 \\ \ddot{q}_3 \\ \ddot{q}_4 \end{pmatrix} = \frac{1}{2} \begin{pmatrix} q_4 & -q_3 & q_2 & q_1 \\ q_3 & q_4 & -q_1 & q_2 \\ -q_2 & q_1 & q_4 & q_3 \\ -q_1 & q_2 & -q_3 & q_4 \end{pmatrix} \begin{pmatrix} \dot{\omega}_x^b \\ \dot{\omega}_y^b \\ \dot{\omega}_z^b \\ -2 \sum_{i=1}^4 \dot{q}_i^2 \end{pmatrix} \quad (\text{Eq. 6})$$

We see that angular accelerations are required in (Eq. 6), and we will see that they are also needed for the first order formulation as well:

$$\begin{aligned} \dot{\omega}_x^b &= \frac{\tau_x^b}{I_{xx}} + \left(\frac{I_{yy} - I_{zz}}{I_{xx}} \right) \omega_y^b \omega_z^b \\ \dot{\omega}_y^b &= \frac{\tau_y^b}{I_{yy}} + \left(\frac{I_{zz} - I_{xx}}{I_{yy}} \right) \omega_z^b \omega_x^b \\ \dot{\omega}_z^b &= \frac{\tau_z^b}{I_{zz}} + \left(\frac{I_{xx} - I_{yy}}{I_{zz}} \right) \omega_x^b \omega_y^b \end{aligned} \quad (\text{Eq. 7})$$

where I_{xx} , I_{yy} , and I_{zz} represent the principal moments of inertia (elements of the diagonalized moment of inertia tensor), τ_x , τ_y , and τ_z represent the net or total torques on the object, and the superscript "b" indicates that these quantities must be expressed in the body fixed (object-local) coordinate system.

Transformation between the body fixed and space fixed coordinate systems is accomplished by means of the transition matrix, \tilde{A} :

$$\tilde{A} = 2 \begin{pmatrix} q_1^2 + q_4^2 - \frac{1}{2} & q_1 q_2 - q_3 q_4 & q_1 q_3 - q_2 q_4 \\ q_1 q_2 - q_3 q_4 & q_2^2 + q_4^2 - \frac{1}{2} & q_2 q_3 - q_1 q_4 \\ q_1 q_3 - q_2 q_4 & q_2 q_3 - q_1 q_4 & q_3^2 + q_4^2 - \frac{1}{2} \end{pmatrix} \quad (\text{Eq. 8})$$

where $\tilde{A}^{-1} = \tilde{A}^T$. For example, a three dimensional vector, r , in space fixed coordinates can be calculated from body fixed coordinates using:

$$e^s = \mathbf{A}^{-1} e^b = \mathbf{A}^T e^b \quad (\text{Eq. 9})$$

and the body fixed torques required in (Eq. 7) are found:

$$\tau^b = \mathbf{A} \tau^s \quad (\text{Eq. 10})$$

METHOD

As mentioned above, we will consider two mathematically equivalent yet procedurally different formulations to numerically solve the classical free body problem. We will initially consider a first order Lagrangian formulation, and then a second order Newtonian formulation. Among the many choices of integration methods, the simple (mom-iterative) Gear method has been chosen, as it is stable, reliable, and conveniently adapted for both first and second systems of differential equations. Once initial conditions, and interaction potential, and the geometry of the moving object (expressed in terms of body fixed offsets from the center of mass) is specified, solution of the free body problem consists of three steps: Predicting, Evaluating, and Correcting.

FIRST ORDER METHOD

The Lagrangian or first order method, a.k.a. Evans method, expresses the equations of motion into sets of first order differential equations. Specifically, this means that for translational motion we will be solving independently for center of mass positions and momenta (and their higher derivatives) and for rotation we will be solving independently for quaternions and angular velocities (and their higher derivatives). The Lagrangian method has certain advantages, namely, since velocities appear explicitly in the equations of motion, it is convenient to impose artificial constraints of the motion (e.g., maintain the system at some target temperature).

Prediction

The prediction step is trivial; a simple Taylor series expansion is written for the translation variables (center of mass position and momenta) and their higher derivatives and for the rotation variables (quaternions and angular velocities) and their higher derivatives. For example, the “x” component of the angular velocity vector could be expressed as follows: (truncating 5th and higher order derivatives):

$$\begin{aligned} x_p &= x + \dot{x}\Delta t + \ddot{x}\frac{\Delta t^2}{2!} + \dddot{x}\frac{\Delta t^3}{3!} + x^{(IV)}\frac{\Delta t^4}{4!} \\ \dot{x}_p &= \dot{x} + \ddot{x}\Delta t + \dddot{x}\frac{\Delta t^2}{2!} + x^{(IV)}\frac{\Delta t^3}{3!} \\ \ddot{x}_p &= \ddot{x} + \dddot{x}\Delta t + x^{(IV)}\frac{\Delta t^2}{2!} \\ \dddot{x}_p &= \dddot{x} + x^{(IV)}\Delta t \end{aligned} \quad (\text{Eq. 11})$$

A similar set of equations would be written for y , z , P_x , P_y , P_z , q_1 , q_2 , q_3 , q_4 , ω_x , ω_y and ω_z .

Evaluation

These Taylor series expansions are now corrected by performing actual system calculations. The first step is to calculate the site coordinates of the object from the predicted center of mass positions and quaternions. (For example, if our object were a water molecule, we would need to calculate the oxygen and hydrogen positions using the four quaternion values and the center of mass position). This is a simple algebraic calculation using (Eq.9) where we calculate space fixed offsets of each site using the body fixed offsets (constants read in as input data) and the transition matrix. These values are then added to the predicted center of mass positions to give predicted positions of each site on the moving object.

The next step is to calculate the forces acting on each site, calculate the total or net force acting on the object, and then calculate the net torque acting on the object. This calculation requires knowledge of how the object interacts with other objects in the system. For example, if modeling planetary motion, the force would be calculated from the laws of gravity. If modeling a system of molecules, then there would need to be some way of expressing the intermolecular interactions in some simple algebraic form. Once all of the site forces have been calculated one can calculate the net torque on the object directly:

$$\tau = \sum_{j=1}^N (r_j \times F_j) \quad (\text{Eq. 12})$$

where N represents the total number of sites on the moving object. These forces will necessarily be in the space fixed frame, but we have seen that these must be referenced to the body fixed coordinate system to be used in (Eq. 7), therefore we use (Eq. 10) to make the transformation.

We next calculated the angular acceleration using (Eq. 7). At this point, the literature states (Allen, et al. 1987) that we should not calculate quaternion velocities using (Eq. 5). This is an error. The angular velocities should be corrected first before evaluating the quaternion velocities. This will be discussed subsequently.

Correction

Positions are corrected using the difference between predicted momenta and predicted velocities:

$$Cor_x^{pos} = \left(\frac{P_x}{m} - \dot{x} \right) \Delta t \quad (\text{and similar for } y \text{ and } z) \quad (\text{Eq. 13})$$

Momenta are corrected based upon the difference between the calculated force and the first derivative of the momenta:

$$Cor_x^{mom} = (F_x - \dot{P}_x) \Delta t \quad \text{and similar for } y \text{ and } z \quad (\text{Eq. 14})$$

Angular velocities are corrected using the difference between the angular acceleration calculated using (Eq. 7) and that predicted in the prediction step:

$$Cor_x^{\omega} = (\dot{\omega}_x^{Calc} - \dot{\omega}_x^{p}) \Delta t \text{ and similar for } y \text{ and } z \quad (\text{Eq. 15})$$

We now evaluate quaternion velocities using (Eq. 5) with the angular velocities from (Eq.15). This enable the final correction step for the quaternions which is based on the difference between quaternions which is based on the difference between quaternion velocities from (Eq. 15) and those resulting from the prediction step:

$$Cor_1^{Q_{nat}} = (\dot{q}_1^{Calc} - \dot{q}_1^p) \Delta t \text{ and similar for } q_2, q_3 \text{ and } q_4 \quad (\text{Eq. 16})$$

According to the Gear predictor-corrector algorithm, these corrections are applied using a set of empirical parameters. First order Gear parameters (Allen et al. 1987) when truncating at the 5th derivative are shown in Table 1.

TABLE 1. Gear parameters for first order system

α_0	251/720
α_1	1
α_2	11/12
α_3	1/3
α_4	1/24

For the x component of the position, the corrector is applied as follows:

$$\begin{aligned} x &= x + \alpha_0 Cor_x^{Pos} \\ \dot{x} &= \dot{x} + \alpha_1 Cor_x^{Pos} \frac{1}{\Delta t} \\ \ddot{x} &= \ddot{x} + \alpha_2 Cor_x^{Pos} \frac{2!}{\Delta t^2} \\ \dddot{x} &= \dddot{x} + \alpha_3 Cor_x^{Pos} \frac{3!}{\Delta t^3} \\ x^{(IV)} &= x^{(IV)} + \alpha_4 Cor_x^{Pos} \frac{4!}{\Delta t^4} \end{aligned}$$

with analogous expressions for y, z, P_x , P_y , P_z , q_1 , q_2 , q_3 , q_4 , ω_x , ω_y and ω_z .

SECOND ORDER METHOD

The second order or Newtonian formulation, a.k.a. the Rapaport method, has the advantage of being simpler and the disadvantage of not having momenta and angular velocities explicit within the integration algorithm.

Prediction

The prediction step is identical to that for the first order implementation above, except that the Taylor series were truncated at the 6th order term. Only two quantities occur: the positions and the quaternions. The momenta and angular velocities must be calculated outside and independent of the integration algorithm.

Evaluation

The site coordinates of the moving object are calculated followed by an evaluation of the site forces, total forces and torques as above. The quaternion accelerations are then calculated using (Eq. 6).

Correction

The predicted positions are corrected based on the difference between the calculated force (divided by the mass) and the predicted accelerations:

$$Cor_x^{Pos} = \left(\frac{F_x}{m} - \ddot{x} \right) \frac{\Delta t^2}{2} \text{ and similar for } y \text{ and } z \quad (\text{Eq. 17})$$

The quaternions are corrected using the difference between the predicted and calculated quaternion accelerations:

$$Cor_1^{Quat} = (q_1^{Calc} - \ddot{q}_1^P) \frac{\Delta t^2}{2} \text{ and similar for } q_2, q_3 \text{ and } q_4 \quad (\text{Eq. 18})$$

First order Gear coefficients (Allen et al. 1987) for truncation at the 6th term are given in Table 2:

TABLE 2. Gear parameters for second order system

β_0	3/16
β_1	251/360
β_2	4
β_3	11/18
β_4	1/6
β_5	1/60

and applied as follows for the x position component:

$$\begin{aligned} x &= x + \beta_0 Cor_x^{Pos} \\ \dot{x} &= \dot{x} + \beta_1 Cor_x^{Pos} \frac{1}{\Delta t} \\ \ddot{x} &= \ddot{x} + \beta_2 Cor_x^{Pos} \frac{2!}{\Delta t^2} \\ \ddot{\ddot{x}} &= \ddot{\ddot{x}} + \beta_3 Cor_x^{Pos} \frac{3!}{\Delta t^3} \\ x^{(IV)} &= x^{(IV)} + \beta_4 Cor_x^{Pos} \frac{4!}{\Delta t^4} \end{aligned}$$

$$x^{(v)} = x^{(v)} + \beta_5 \text{Cor}_x^{\text{Pos}} \frac{5!}{\Delta t^5}$$

with analogous expressions for y , z , q_1 , q_2 , q_3 and q_4 .

TEST CASES AND DISCUSSION

We consider a four-site dynamic body, perhaps a molecule, a space vehicle, etc. as shown in Figure 1. The body consists of four spheres, the smallest two (spheres 1 and 2), a diameter of 1 unit each, the next largest (spheres 3), a diameter of 4 units, and the largest (sphere 4), a diameter of 10 units.

If we arbitrarily consider sphere 3 to be the origin of a body fixed coordinate system, we find that the center of mass position as the new origin, we calculate the moment of inertia tensor to be:

$$\begin{pmatrix} 1635 & 0 & 0 \\ 0 & 1611 & 150 \\ 0 & 150 & 96 \end{pmatrix}$$

A slight rotation (finding the eigenvalues of the tensor) yields the principal moments of inertia required in (Eq. 7):

$$\begin{pmatrix} 1635 & 0 & 0 \\ 0 & 1625.71 & 0 \\ 0 & 0 & 81.29 \end{pmatrix}$$

The object described above was taken to interact with a fixed 'cage' consisting of 26 spheres which comprise an empty cube with a half length of 100 units and centered about the origin. It was arbitrarily chosen to have the spheres of the cage and the spheres comprising the mobile object interact with each other sphere and Coulombic interactions:

$$U(r) = 4\epsilon \left[\left(\frac{\sigma}{r} \right)^{12} - \left(\frac{\sigma}{r} \right)^6 \right] + \frac{q_{\text{cage}} q_{\text{site}}}{r} \quad (\text{Eq. 19})$$

where r is the distance between the cage site and any one of the four object sites. q refers to the electronic charge assigned to the cage sites and to each of the four sites of the mobile object. The depth of potential energy "well" is given by e and the sphere diameter is given by s . Forces are calculated simply by taking the negative gradient of (eq. 19). This potential model provides regions of space with both negative and infinitely positive (overlap) potential energies. When objects with different interaction parameters are involved, we used arbitrary combining rules to determine 'effective' parameters:

$$\sigma_{\text{eff}} = \frac{\sigma_1 + \sigma_2}{2} \quad \text{and} \quad \epsilon_{\text{eff}} = \sqrt{\epsilon_1 \epsilon_2} \quad (\text{Eq. 19a})$$

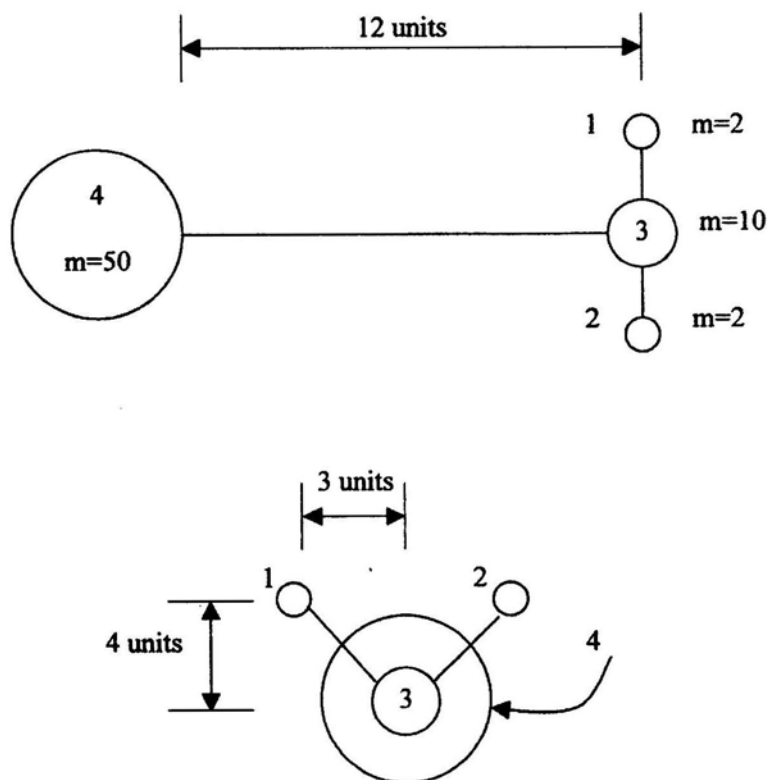


FIGURE 1. Front view and side view of the moving object

Site properties in dimensionless units for the mobile object are summarized in Table 3.

TABLE 3. Site summary for mobile object

	Sphere 1	Sphere 2	Sphere 3	Sphere 4
mass	2	2	10	50
diameter	1	1	4	10
charge	-0.25	-0.25	-0.5	+1.0
well depth (e)	0	0	0	10

A site summary for the stationary fixed cage particles is given in Table 4.

TABLE 4. Site summary for fixed objects

	Spheres
mass	∞
diameter	10
charge	± 1
well depth (e)	10

The choice of initial conditions will determine the behavior of the system. If conditions are chosen such that the total energy is negative, then it is impossible for the object to venture far from the fixed particles. If these conditions are fixed, however, so that the total energy is positive, then the object may leave the system never to return.

Test case 1

Run conditions for Test case one are given in Table 5 where all second and higher order derivatives have been set to zero.

TABLE 5. Run conditions for test case 1

Δt	0.0001
x_0	84.0
y_0	0
z_0	0
ϕ	40°
Ψ	100°
θ	85°
\dot{x}	0.2
\dot{y}	0
\dot{z}	0
ω_x	+ 0.05 π /8
ω_y	- 0.05 π /4
ω_z	+ 0.05 π /8

The total energy is the sum of translational kinetic energy, rotational kinetic energy, and potential or configurational energy:

$$E_{tot} = \frac{1}{2}m\dot{x}^2 + \frac{1}{2}m\dot{y}^2 + \frac{1}{2}m\dot{z}^2 + \frac{1}{2}I_{xx}\omega_x^2 + \frac{1}{2}I_{yy}\omega_y^2 + \frac{1}{2}I_{zz}\omega_z^2 + \sum_{i=1}^{26} u_{i,obj} \quad (\text{Eq. 20})$$

where the last term indicates a summation of the interactions between the moving object and the 26 fixed spheres comprising the cage. The total energy for this test case is -0.7236 units.

Figure 2 shows the total kinetic (rotational + translational) energy, potential energy, and total energy for the first order method for the first 50 million time steps. One observes that the energy conservation is excellent and holds tightly to the total energy vary enormously. Figure 3 shows an identical run, but employing the second order method. Close examination of these figures reveals an interesting observation. We see that although the energy is conserved tightly using either method, that system behavior is quite different after approximately 1 million time steps (after $t = 1000$ units).

This is shown more clearly in Figure 4 where we observed the value of the x - coordinate over the run duration. First and second order x - coordinate trajectories are both plotted on Figure 4 and we see that the two curves are coincident until around $t = 1300$ or approximately 1.3 million time steps. The two algorithms produced identical results for the first 1.3 million time steps, after which we see unique behavior of the two systems. By $t = 1500$

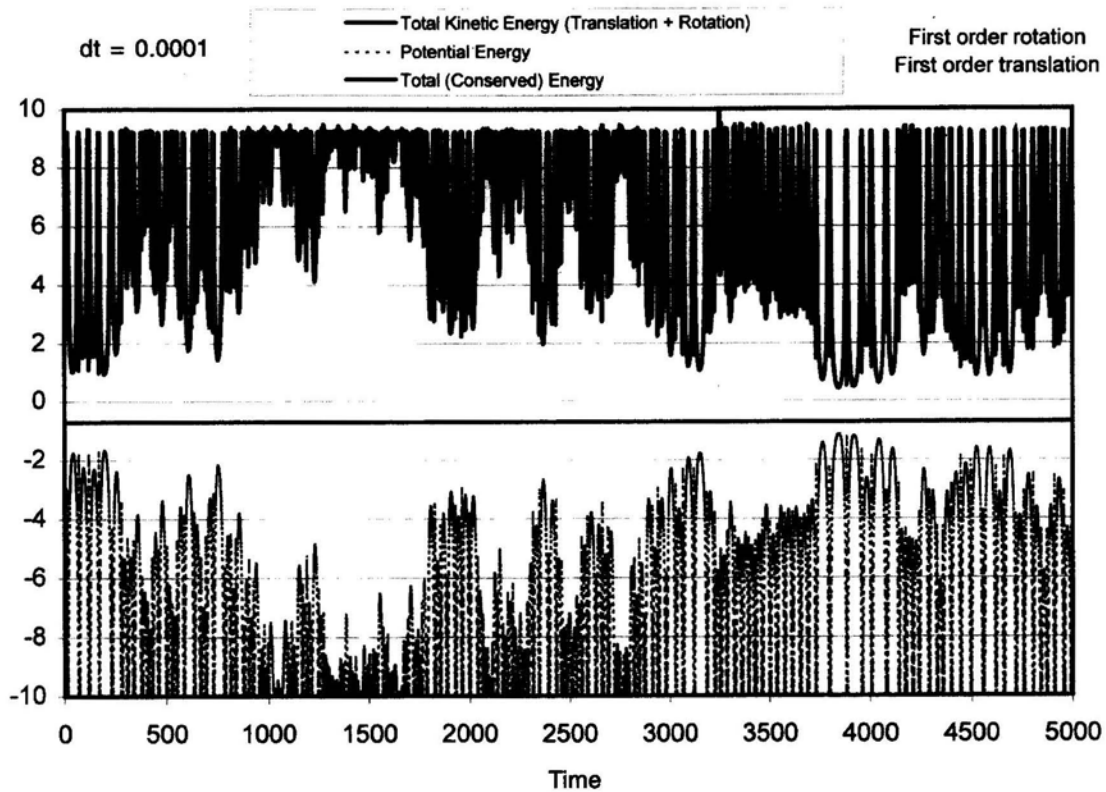


FIGURE 2. Potential, kinetic, and total energy for the first order method

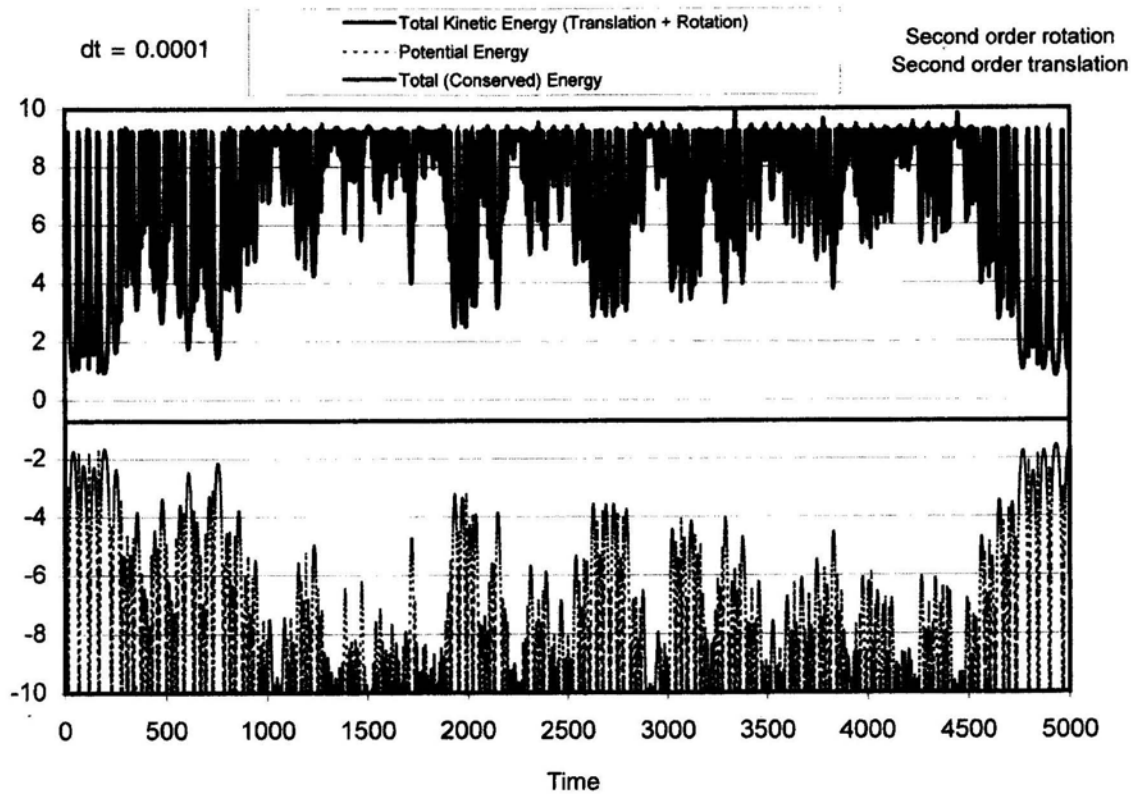


FIGURE 3. Potential, kinetic, and total energy for the second order method

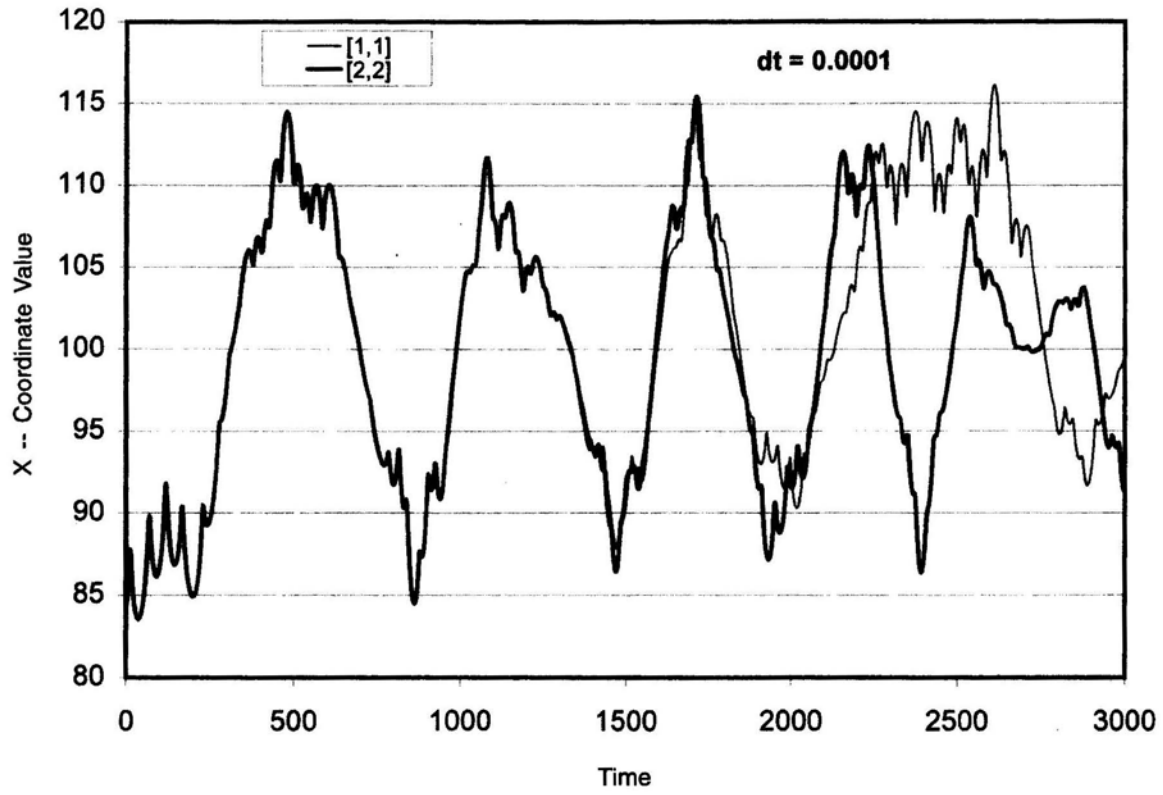


FIGURE 4. x - component of object trajectory

this unique behavior is easily observable, by $t = 2500$, our moving object appears to be on two different trajectories. In both cases we observed that the mobile object is orbiting one of the fixed spheres. Since the total energy is negative, it does not possess the 'escape velocity' to leave the orbits of the fixed spheres.

Test case 2

Run conditions for test case 2 are identical to those above except that a much larger time step were used, $\Delta t = 0.125$. The total run involves only 40000 time steps. Figure 5 and 6 shows the energy profiles for the first and second order formulations, respectively. We notice the upwards energy drift which occurs at around $t = 4000$ for the first order case. This is not evident in Figure 6, though we conclude that this is a too large of time step to produce accurate results. Furthermore, from Figure 7 (analogous to Figure 4 above), we see the two methods produce coincident results only for the first 2000 or so time steps (i.e., until about $t = 300$). These first 2000 time steps are also identical to the results for Test case 1. We also observed that the first order curve on Figure 1 is similar to its counterpart on Figure 4 to approximately $t = 1000$.

Test case 3

Test case 3 employs initial conditions such that the total energy is positive ($E_{tot} = +3.993$ units) and hence the possibility to exist that the mobile object will break orbit and leave the system. Table 6 shows initial and run conditions.

TABLE 6. Run conditions for test case 3

Δt	0.0005
x_0	70
y_0	0
z_0	0
ϕ	40°
Ψ	100°
θ	85°
\dot{x}	0
\dot{y}	0
\dot{z}	0
ω_x	+ 0.08 π /8
ω_y	- 0.08 π /4
ω_z	+ 0.08 π /8

Initially the kinetic energy is contributed entirely by rotational motion. Translational, rotational, and total kinetic energy over the run is shown in Figure 8 and Figure 9 for first and second order formulations, respectively. Since our object lies near a fixed cage body the potential energy interactions quickly (by $t = 20$) induce center of mass translation. The object interacts with the cage before leaving the system entirely, after which the potential energy approaches zero and kinetic energy is distributed between rotational and translational degrees of freedom. This is observed in Figure 10 and 11

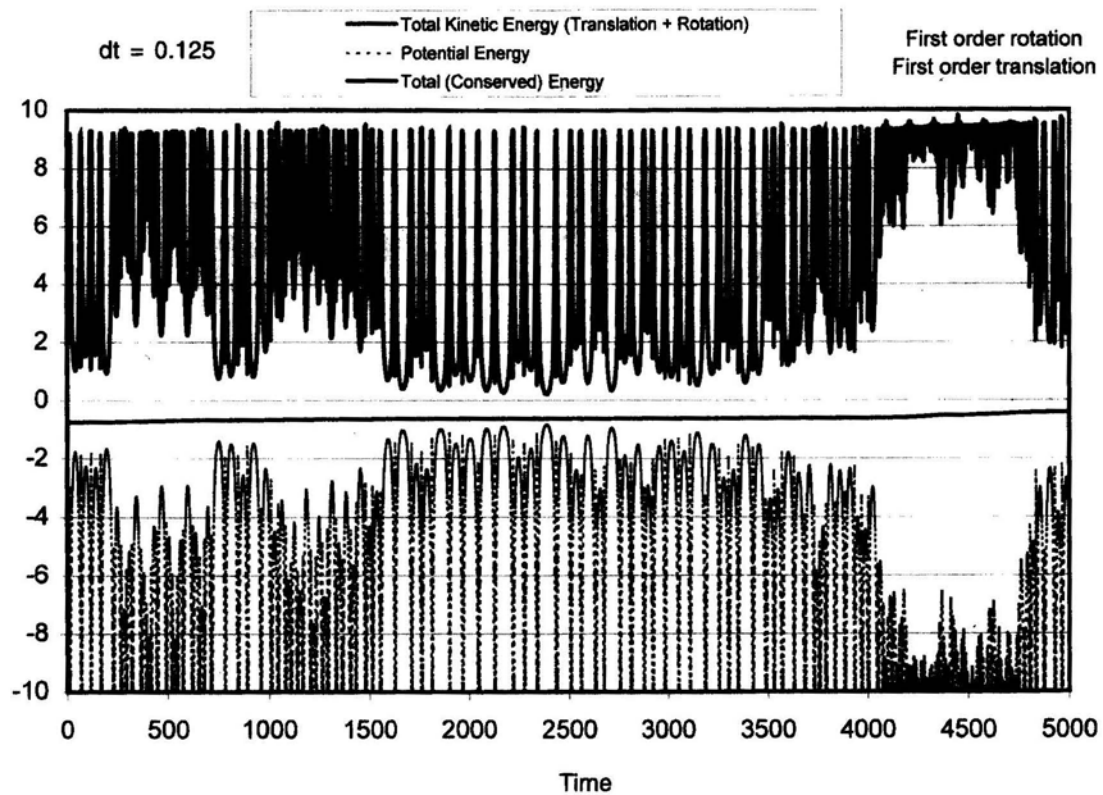


FIGURE 5. Potential, kinetic, and total energy for the first order formulation

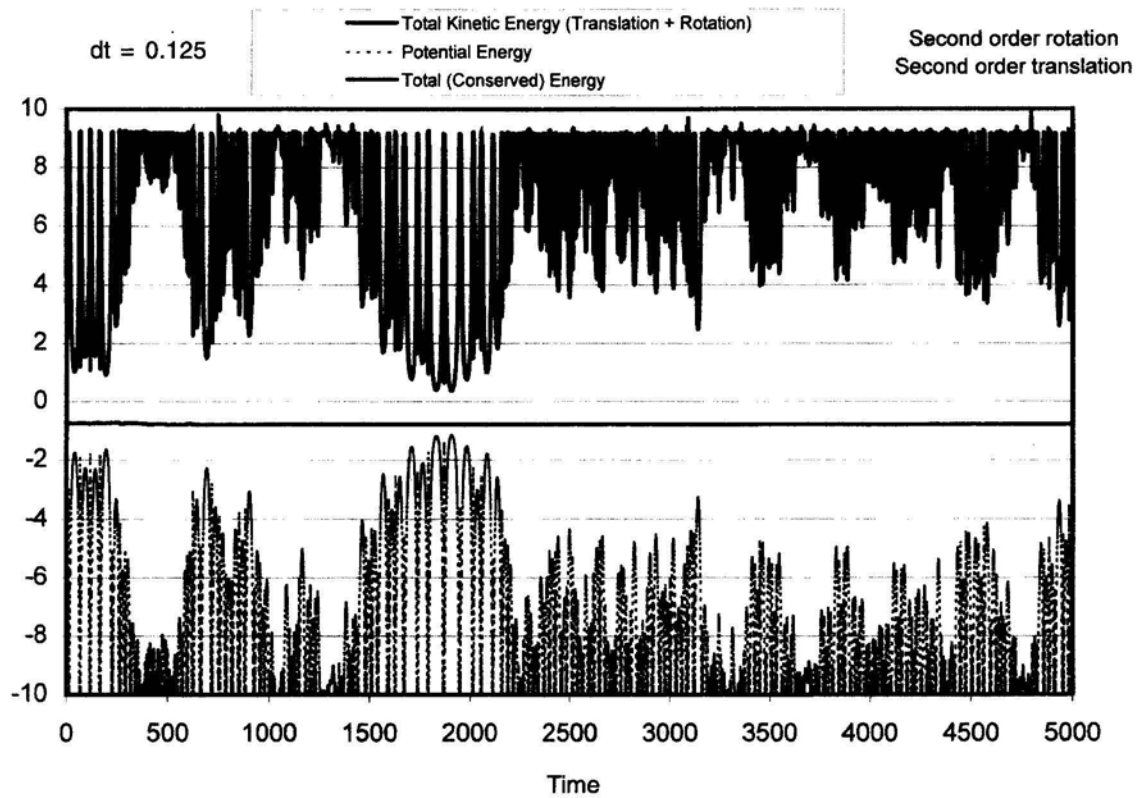


FIGURE 6. Potential, kinetic, and total energy for the second order formulation

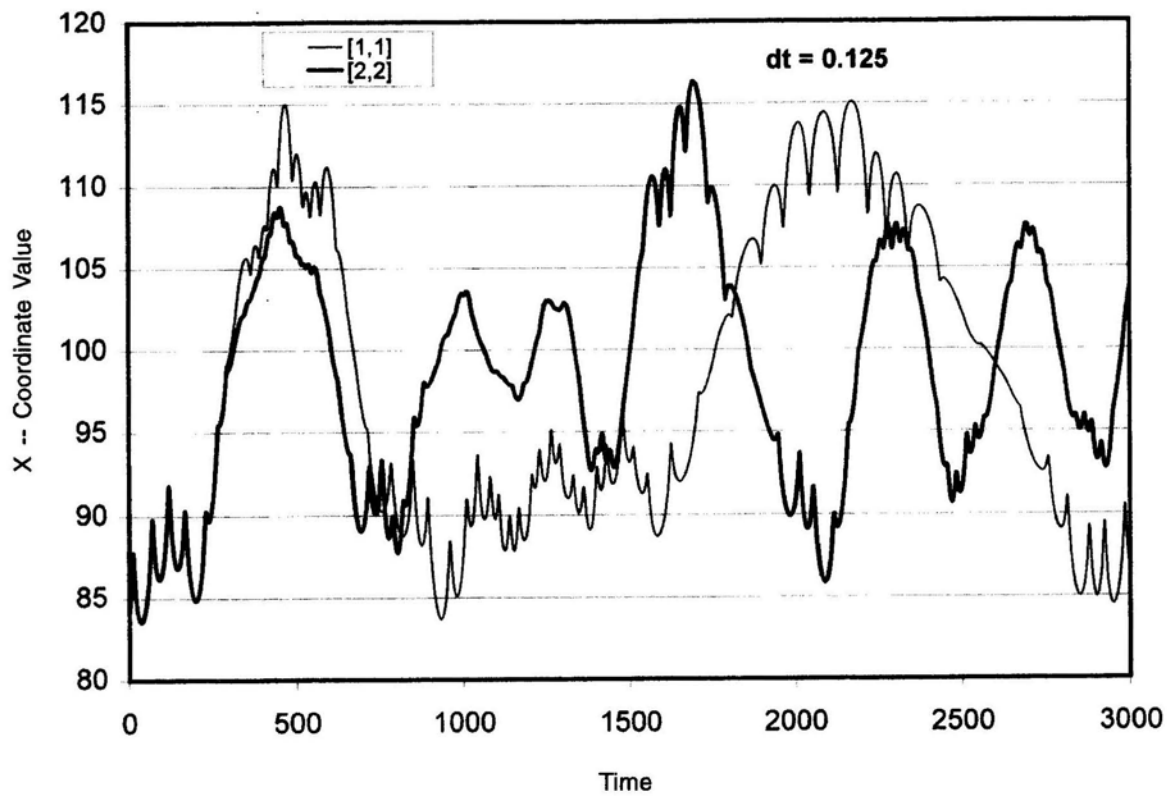


FIGURE 7. x - component of object trajectory

dt = 0.005

— Translational Kinetic Energy
— Rotational Kinetic Energy
— Total Kinetic Energy

First order rotation
First order translation

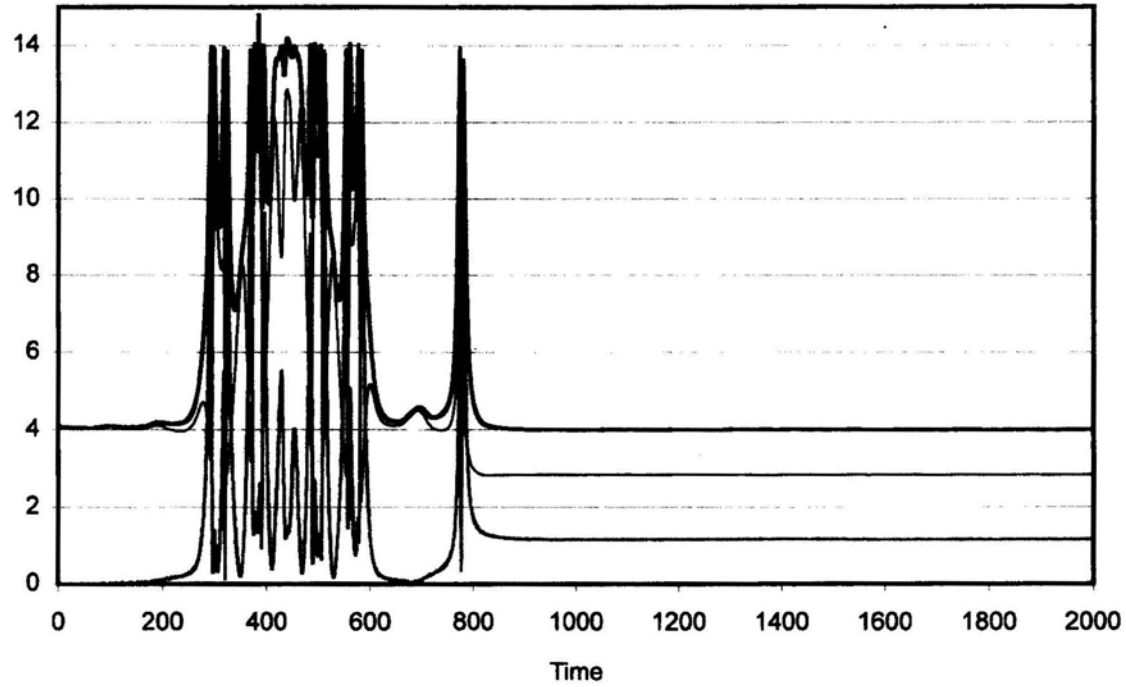
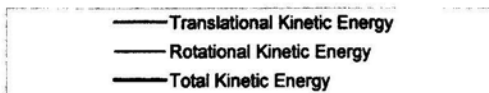


FIGURE 8. Translational, rotational, and total kinetic energy for the first order formulations

dt = 0.005



Second order rotation
Second order translation

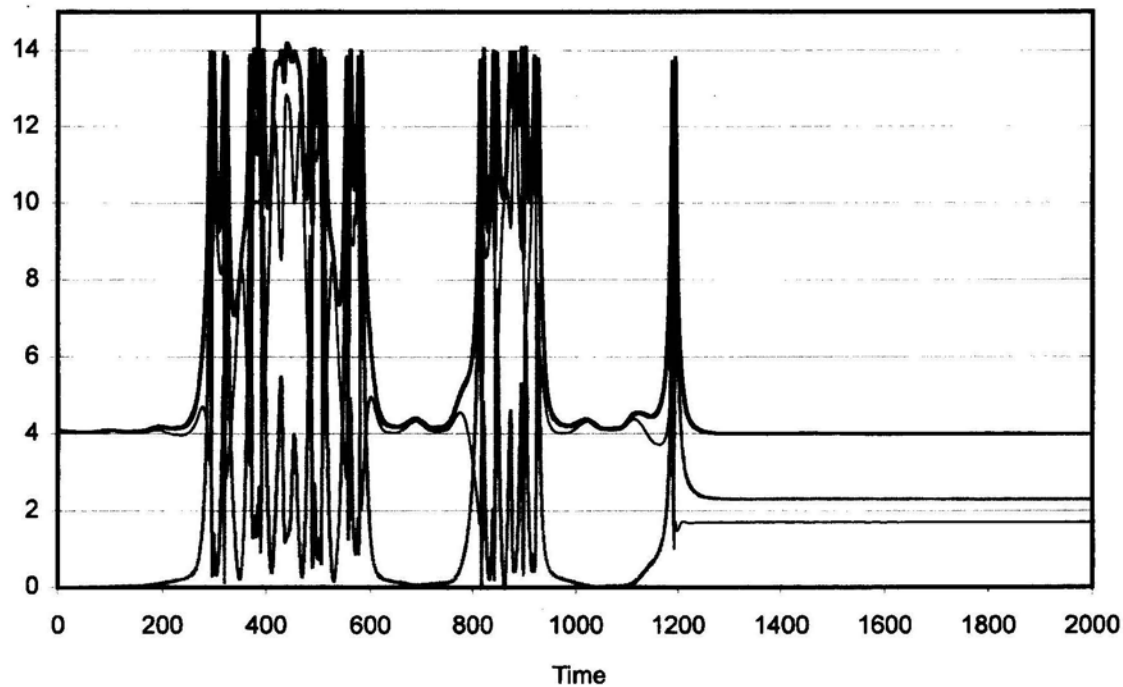


FIGURE 9. Translational, rotational, and total kinetic energy for the second order formulations

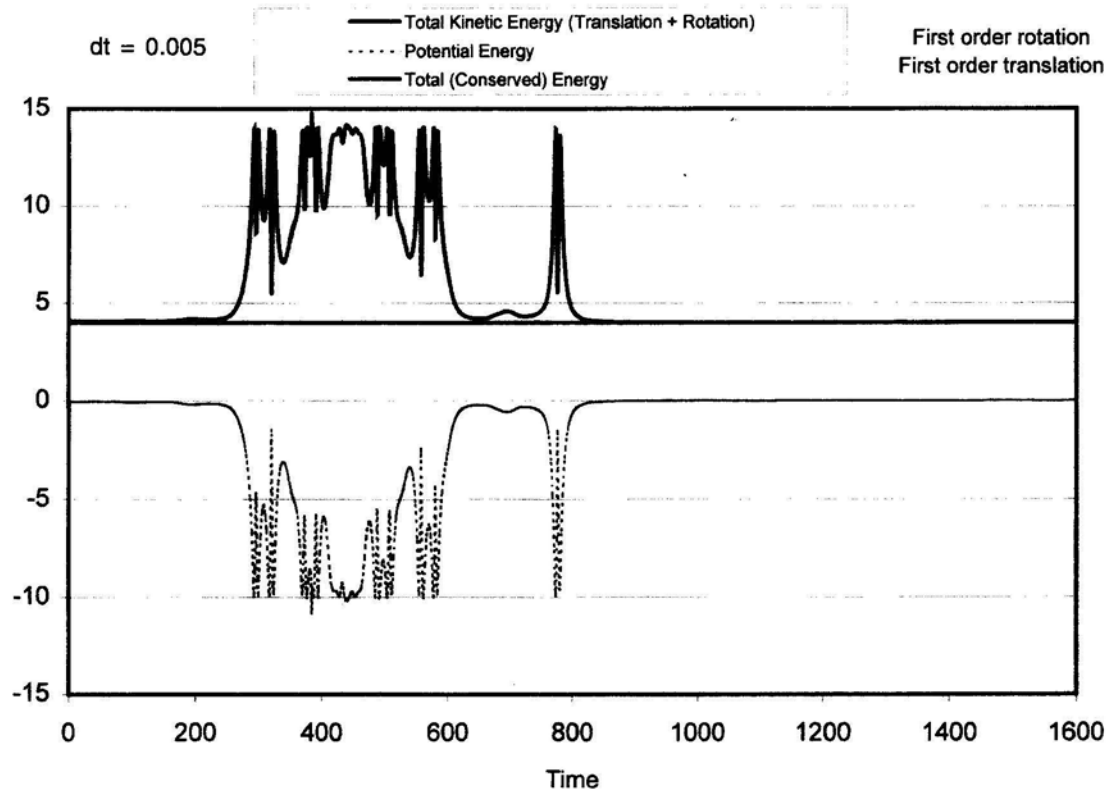


FIGURE 10. Potential, kinetic, and total energy

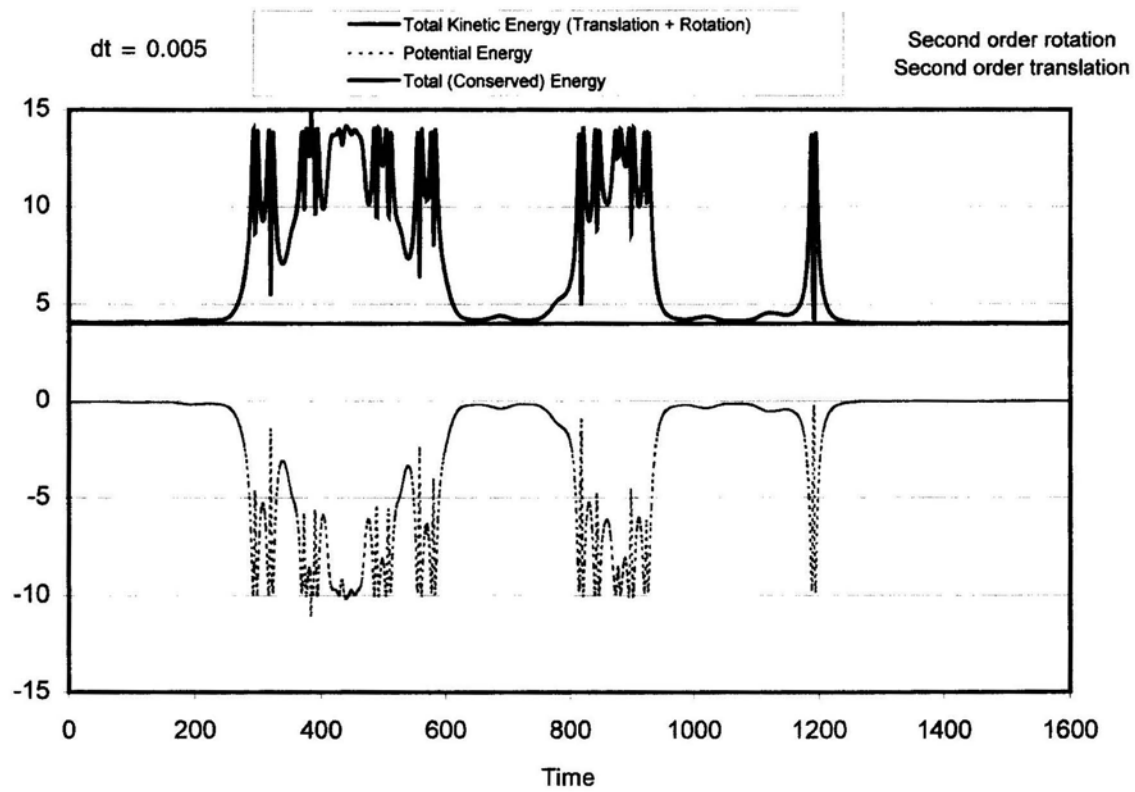


FIGURE 11. Development of potential, kinetic, and total energy throughout the run

which show development of total kinetic energy, potential energy, and total energy throughout the run. We observed after $t = 800$ (about 160000 time steps) that the first and second order formulations give different solutions. This is further shown in Figures 12 and 13, where we observed that our first order object leaves the system in the negative z direction whereas the second order object leaves the system in the positive y direction.

DISCUSSION

We have observed the first and second order formulations of the three body problem are able to yield identical results over a period of time, and the time at which solutions begin to differ depends on the size of the time step. These observations are summarized in Table 7.

TABLE 7. Time steps before first and second order solutions begin to differ

Δt	Time steps
0.001	1,300,000
0.005	160,000
0.125	2000

What is happening here? Are the algorithms in error or is there an error in coding? It is believed not, and for the following reasons.

1. Both algorithms yield identical solutions over many thousands of time steps;
2. Both algorithms tightly maintain energy conservation with no arbitrary velocity rescaling;
3. Within the confines of Table 7, the same solutions are found using various values for the time increment;
4. The solutions are physically realistic and yield similar results in both FORTRAN and C++ and give correct solutions for simplified one and two dimensional test cases. (Khairil 2000)
5. Both algorithms have been used extensively in molecular modeling.

Unfortunately, computers deal with numbers of finite precision and these numerical algorithms are exact only on the limit of ($t = 0$). The trajectories are therefore rendered unstable after times sufficiently long for accumulation of error. This means an infinitesimally small perturbation introduced in the system will remain masked for some time, but will eventually cause the trajectory to drift away from its parent trajectory.

It is not necessarily undesirable for these trajectories to become unstable, as in many applications we desire to approach some steady state or equilibrium state, and it is necessary that the equilibrium state be uncorrelated with starting conditions. Hence these algorithms have been used in calculation of thermodynamic properties.

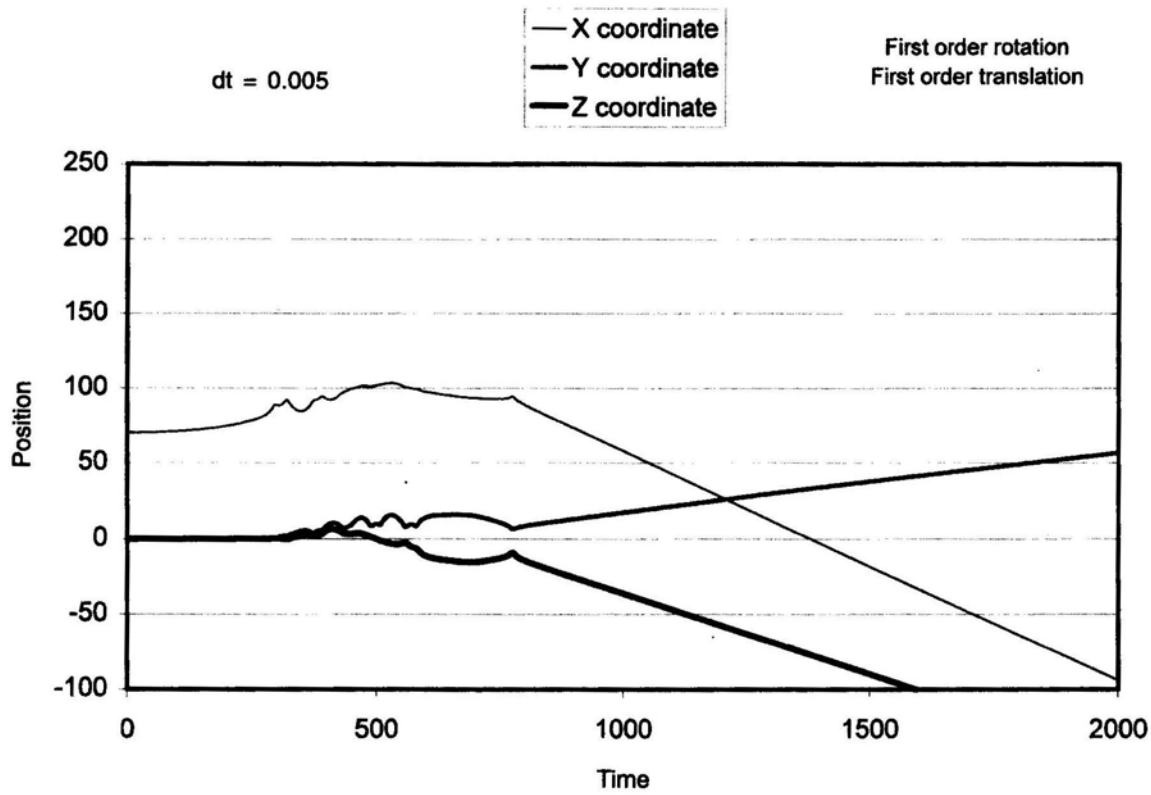


FIGURE 12. x, y, and z - trajectory components

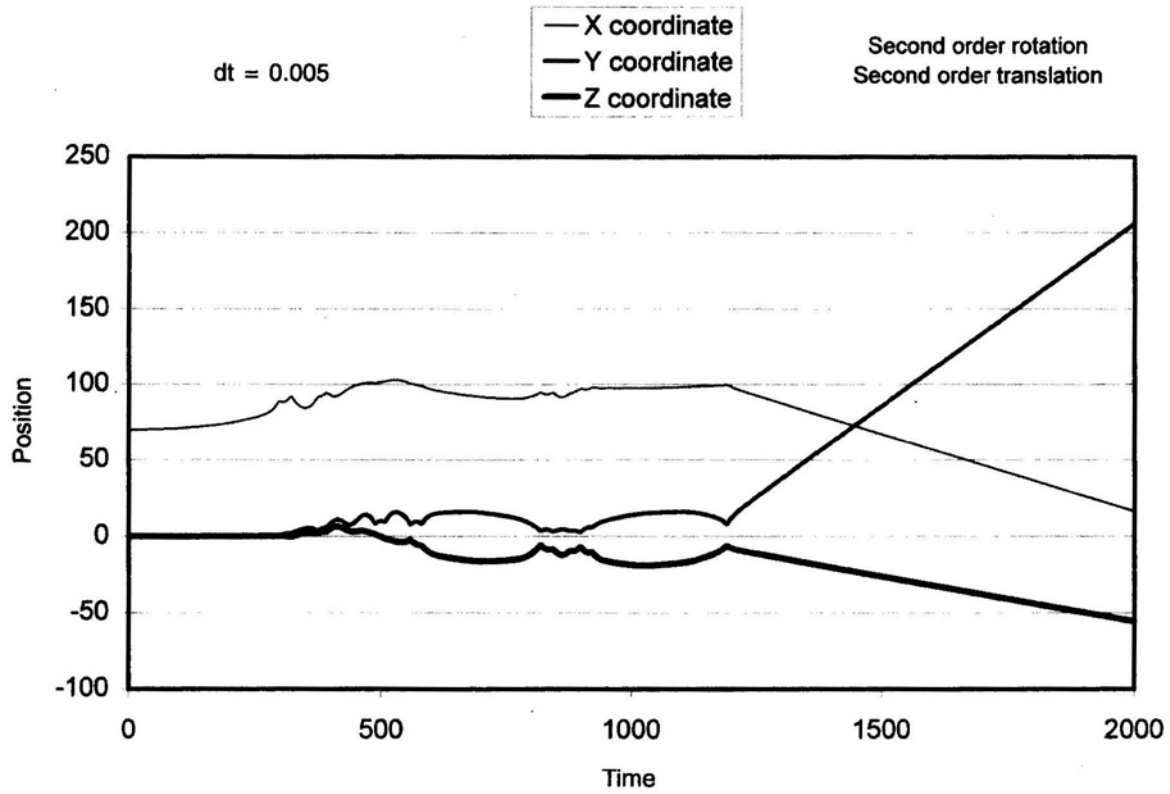


FIGURE 13. x, y, and z - trajectory components

CONCLUSIONS

Both the Evans and Rapaport algorithms provide general and flexible methods for modeling free body motion. These algorithms are useful and powerful enough they should be known and appreciated by those outside the area of molecular simulation. Within computer truncation error and error associated with the numerical methods themselves, these algorithms will yield exact solutions for the supplied potential interactions. Providing an accurate model for these potential interactions is the weak point in both microscopic and macroscopic modeling of free body motion.

REFERENCES

- Allen, M. P., Tildesley, D. J., *Computer Simulation of Liquids*. Oxford: Clarendon Press.
- Evans, D. J., 1977, On the Representation of Orientation Space. *Mol. Phys.*, 34 (2): 317-323.
- Evans, D. J., 1983, Computer 'Experiment' for Nonlinear Thermodynamics of Couette Flow. *J. Chem. Phys.* 78 (1): 3297-3301.
- Goldstein, H., 1980. *Classical Mechanics*. Reading: Addison-Wesley.
- Haile, J. M., 1992. *Molecular Dynamics Simulation, Elementary Methods*. New York: Wiley Interscience.
- Khairil Mazwan, 2000. Peramal Gear Tertib Ke-2 - Kaedah Pembedulan Bagi Gerakan 3 Dimensi Molekul Tegar. Thesis Universiti Kebangsaan Malaysia, Department of Chemical and Process Engineering.
- Rapaport, D. C., 1985. Molecular Dynamics Simulation Using Quaternions: *J. Comp. Phys.* 60: 306-314.
- Rapaport, D. C., 1998. *The Art of Molecular Dynamics Simulation*. Cambridge: Cambridge University Press.
- Ryckaert, J P., Ciccotti, G., Berendsen, J.C., 1976. Numerical Integration of the Cartesian Equations of Motion of a System with Constraints: Molecular Dynamics of n-Alkenes. *J. Comp. Phys.* 23: 327-334.
- Sonnenschein, R. 1985. An Improved Algorithm for Molecular Dynamics Simulation of Rigid Molecules. *J. Comp. Phys.* 59: 347-351.
- Spiegel, M. R., 1986. *Schaum's Outline Series - Theoretical Mechanics*. Singapore: McGraw Hill.

Ronald M. Pratt
Khairil Mazwan Bin Mohamad Zaini
Chemical Engineering Department
Universiti Kebangsaan Malaysia
43600 UKM Bangi
Selangor D.E., Malaysia
e-mail: rpratt@fresno.edu